

# Effects of Imperfect Blind Channel Estimation on Performance of Linear CDMA Receivers

Zhengyuan Xu, *Senior Member, IEEE*

**Abstract**—In a code division multiple access (CDMA) system, signal detection under multipath distortion typically requires estimation of unknown channel parameters first. In such a scenario, performance of receivers highly relies on the accuracy of channel estimates. In this paper, effects of channel estimation errors on the performance of linear CDMA receivers due to finite data samples are studied when channel parameters are estimated blindly by a recently proposed covariance-matching technique. Those receivers include zero-forcing (ZF), direct matrix-inversion (DMI) minimum mean-square-error (MMSE), subspace MMSE, and RAKE receivers. Their output signal-to-interference-plus-noise ratios (SINRs) and bit-error-rates (BERs) are adopted for performance measures. Expressions for performance indicators under such an imperfect condition are derived from a perturbation perspective and verified by simulation examples.

**Index Terms**—Code-division multiple access, covariance matching, multiuser detection, perturbation analysis.

## I. INTRODUCTION

IN the past decade, communication world has witnessed widespread deployment of direct sequence (DS) code division multiple access (CDMA) systems because of various attractive features of the CDMA technology [1], [2]. This technology enables simultaneous spectrum sharing, mitigation of jamming, interception and multipath fading [3], and transmission of multirate information streams. It will continue to dominate future generation wireless networks [4].

It is known that multiuser interference (MUI) is a typical obstacle to be obviated in detection of input signals in a DS/CDMA system, which has attracted significant attention in recent years [5]. In a DS/CDMA system, bandwidth of input signals is spread by orders of magnitude by a spreading sequence uniquely assigned to individual users. Those spreading sequences facilitate user differentiation and signal detection at the receiver. For example, a decorrelating receiver utilizes spreading codes of all users to separate users' signals. Subspace methods first identify either the signal subspace or noise subspace and then apply waveform projection for channel identification [6], [7]. Those estimated channel parameters can be directly applied to build various linear receivers [8], [9], where spreading codes of the desired user play an important role. As closely related methods, minimum variance or minimum

output energy (MOE) approaches impose proper constraints on receivers based on the structure of the desired waveform, depending on the spreading codes and multipath channel characteristics [10]–[12]. It is shown that performance of channel estimators and receivers depends on projection of the desired code matrix onto both the signal subspace and noise subspace. Successive study shows that improvements can be made in channel estimation and linear detection after introducing a properly selected regularization parameter to the MOE cost function [13], [14]. Recent investigation further closes the gap between the MOE and subspace methods by a so-called power of R (POR) technique [15], [16]. The corresponding method modifies the MOE cost function by raising the power of the data covariance matrix. Although its theoretical equivalence to the subspace technique is established, the POR technique has been shown to be more robust. Significant improvements have been observed in practical situations. The major reason stems from its subspace approximation without subspace decomposition, which is regarded as a soft decision instead of hard decision process [16]. Therefore, it avoids rank estimation and shows robustness to channel order mismatch and other imperfectness. Similar to the MOE technique, projection of the desired user's code matrix onto both the signal and noise subspaces in the POR technique affects the detection performance. Covariance matching is another technique directly based on the data covariance and spreading codes [17]. All spreading codes are utilized for simultaneous estimation of channel parameters of active users.

Most multiuser detection and channel estimation techniques are developed under perfect conditions first and then applied to practical scenarios to test performance degradation and robustness. Since various imperfectness may stem from many sources such as background noise, finite sample size, not *a priori* known channel order, synchronization error, user variation, etc., performance prediction under those errors is necessary to better evaluate individual method. For example, sensitivity of multiuser detectors' performance to channel mismatch is analyzed in [18], when transmitted signals suffer from flat fading. Subspace-based multipath channel estimation errors for a multirate CDMA system are derived for given finite number of observations [19]. In [20], perturbation to subspace decomposition of a matrix is studied when errors are introduced to the matrix by either noise or finite sample size. In general, error analysis is feasible for most methods applied in a real world when error can be regarded as a perturbation or when distribution of the error event is known. Although channel estimation can assist symbol detection, one of the objectives in communication system design is to build satisfactory receivers for detection of input signals.

Manuscript received May 22, 2003; revised November 7, 2003. This work was supported in part by the U.S. National Science Foundation under Grant NSF-CCR 0207931. The associate editor coordinating the review of this paper and approving it for publication was Dr. Franz Hlawatch.

The author is with the Department of Electrical Engineering, University of California, Riverside, CA 92521 USA (e-mail: dxu@ee.ucr.edu).

Digital Object Identifier 10.1109/TSP.2004.834408

Therefore, performance of receivers pertinent to channel estimators needs to be studied jointly with the channel estimation methods.

In this paper, we analyze four linear CDMA receivers including zero-forcing (ZF), direct matrix-inversion (DMI) minimum mean-square-error (MMSE), subspace MMSE [9], and RAKE receivers when the channel is not perfectly known but estimated blindly by a recently proposed covariance-matching technique [17]. Each receiver's output signal-to-interference-plus-noise ratio (SINR) and bit-error-rate (BER) are adopted for performance measures. Imperfectness from finite sample size is treated as perturbation whose effect is particularly studied. To achieve our goal, statistics of sample covariance are necessary. Although the matrix version in terms of weighted covariance matrix has become available [21], auto-covariance of the vector form and cross-covariance between the matrix form and vector form are needed as well. They are derived in detail in light of [22]. Similar to [21], they can be regarded as general results and possibly applied to analysis of other methods. Then, SINR and BER under such an imperfect condition are analyzed from a perturbation perspective and verified by extensive simulations.

For notational convenience, let us denote Hermitian-complex conjugate by  $(\cdot)^*$ , transpose  $(\cdot)^T$  by  $(\cdot)^H$ , integer ceiling by  $\lceil \cdot \rceil$ , vector 2-norm by  $\|\cdot\|$ , and matrix Frobenius norm by  $\|\cdot\|_F$  [23], trace of a matrix by  $\text{tr}(\cdot)$ , expectation of a random variable by  $E\{\cdot\}$ , the  $a$ th ( $a = 1, 2, \dots$ ) column of a matrix  $\mathbf{U}$  as  $\mathbf{u}_a$ ,  $\mathbf{1}_a$  as a column vector of length  $a$  with all elements equal to one,  $\mathbf{I}_a$  as an identity matrix of degree  $a$  whose  $b$ th column is denoted as  $\mathbf{e}_{a,b}$ , the Kronecker product as " $\otimes$ " [23], a "vec" operation to successively stack columns of a matrix into a big column vector, the matrix Hadamard product " $\odot$ " to represent element wise multiplication, and the Khatri-Rao product " $\square$ " to represent column-wise Kronecker product [24]:  $\mathbf{U}\square\mathbf{W} = [\mathbf{u}_1 \otimes \mathbf{w}_1, \mathbf{u}_2 \otimes \mathbf{w}_2, \dots]$ . The following properties of "vec," " $\otimes$ ," and " $\square$ " are used throughout the paper:

$$\|\mathbf{A}\|_F^2 = \|\text{vec}(\mathbf{A})\|^2 \quad (1)$$

$$\text{vec}(\mathbf{ABC}) = (\mathbf{C}^T \otimes \mathbf{A})\text{vec}(\mathbf{B}) \quad (2)$$

$$(\mathbf{A} \otimes \mathbf{B})(\mathbf{C} \otimes \mathbf{D}) = (\mathbf{AC}) \otimes (\mathbf{BD}) \quad (3)$$

$$(\mathbf{A} \otimes \mathbf{B})(\mathbf{C}\square\mathbf{D}) = (\mathbf{AC})\square(\mathbf{BD}). \quad (4)$$

A diagonal or block diagonal matrix with main diagonal entries  $\mathbf{x}_i$  is denoted as  $\text{diag}\{\mathbf{x}_1, \mathbf{x}_2, \dots\}$ . We also denote a perturbation by preceding the corresponding quantity by  $\delta$  and the perturbed quantity with  $\hat{\cdot}$ . For example,  $\delta\mathbf{g}_j = \hat{\mathbf{g}}_j - \mathbf{g}_j$ ,  $\delta\mathbf{R} = \hat{\mathbf{R}} - \mathbf{R}$ .

The paper has the following structure. A CDMA system model is described in Section II. Covariance-matching based blind channel estimation method is reviewed and implementations of four typical linear detectors are proposed in Section III. In Section IV, performance of channel estimator and different receivers based on finite received data samples and estimated channel parameters is evaluated. Finally, various simulation examples are provided in Section V, and conclusions are drawn in Section VI.

## II. CDMA SYSTEM MODEL

Consider an uplink CDMA system with  $J$  users. User  $j$  ( $j = 1, \dots, J$ ) is assigned periodic spreading codes  $c_j(k)$  ( $k = 1, \dots, P$ ) of length  $P$  to spread its information symbol  $w_j(n)$ . Let its chip sequence be transmitted through a linear time-invariant channel with a baseband discrete-time chip-rate impulse response  $g_j(l)$ . Then, the received discrete-time signal  $y_j(n)$  at the chip-synchronized receiver due to user  $j$  has a form [10]

$$y_j(n) = \sum_{l=-\infty}^{\infty} w_j(l)h_j(n - d_j - lP) \quad (5)$$

where  $w_j(n)$  is assumed to have zero-mean and variance  $\sigma_{w_j}^2$ ,  $h_j(n)$  is a waveform sequence

$$h_j(n) = \sum_{i=-\infty}^{\infty} g_j(i)c_j(n - i) \quad (6)$$

and  $d_j$  is the propagation delay of user  $j$  in chip periods. After considering all  $J$  users and zero-mean additive white Gaussian noise (AWGN)  $v(n)$  whose variance is denoted as  $\sigma_v^2$ , the received signal becomes

$$y(n) = \sum_{j=1}^J y_j(n) + v(n). \quad (7)$$

The discrete-time model can be easily formulated into a matrix/vector representation. For convenience, we assume a quasi-synchronous system with  $d_j \ll P$  and absorb propagation delay into the channel for each user. The maximum delay spread of all multipath channels is  $q$  chips. If we collect  $\nu = MP$  chip-rate samples in a vector  $\mathbf{y}_n$  at the receiver, then we may choose integer  $M$  to satisfy  $MP \geq P + q - 1$  in order to maximally explore path diversity. In a case of  $q \ll P$ ,  $M = 1$  appears as a good choice for low complexity while incurring little degradation in detection performance. The data vector of length  $\nu$  is then given by [10]

$$\mathbf{y}_n = \sum_{j=1}^J \sum_{m=-K}^{M-1} \mathbf{C}_{j,m} \mathbf{g}_j w_j(n+m) + \mathbf{v}_n \quad (8)$$

where  $K = \lceil (q-1)/P \rceil$ ,  $\mathbf{g}_j$  is the channel vector of length  $q$ ,  $\mathbf{C}_{j,m}$  is the code filtering matrix of user  $j$  for symbol  $w_j(n+m)$ , which can be obtained from a  $\nu \times q$  matrix  $\mathbf{C}_{j,0}$  (corresponding to symbol  $w_j(n)$ ) by shifting it up (if  $m < 0$ ) or down (if  $m > 0$ ) by  $|m|P$  rows

$$\mathbf{C}_{j,0} = \begin{bmatrix} c_j(1) & & \mathbf{0} \\ \vdots & \ddots & c_j(1) \\ c_j(P) & & \vdots \\ \mathbf{0} & \ddots & c_j(P) \\ \mathbf{0} & \dots & \mathbf{0} \end{bmatrix}, \quad \mathbf{g}_j = \begin{bmatrix} g_j(1) \\ \vdots \\ g_j(q) \end{bmatrix} \quad (9)$$

and  $\mathbf{v}_n$  is the noise component. In (8), there exists intersymbol interference (ISI) induced by multipath channel. The total number of symbols contributed to  $\mathbf{y}_n$  by each user is  $M + K$ . For conciseness, the vector form model (8) can be written as

$$\mathbf{y}_n = \mathbf{H}\mathbf{w}_n + \mathbf{v}_n \quad (10)$$

where  $\mathbf{H}$  is called a signature waveform matrix

$$\begin{aligned} \mathbf{H} &= [\mathbf{H}_1, \dots, \mathbf{H}_J] \\ \mathbf{H}_j &= [\mathbf{C}_{j,-K}\mathbf{g}_j, \dots, \mathbf{C}_{j,M-1}\mathbf{g}_j] = \mathbf{C}_j(\mathbf{I}_{M+K} \otimes \mathbf{g}_j) \end{aligned} \quad (11)$$

$\mathbf{C}_j$  is a column-wise concatenation of all code filtering matrices of user  $j$ , and  $\mathbf{w}_n$  contains all  $L = J(M+K)$  inputs contributed to the received data vector  $\mathbf{y}_n$ . From the column index  $a$  ( $a = 1, \dots, L$ ) of  $\mathbf{H}$ , we can easily determine the corresponding user index as  $j_a = \lceil a/(M+K) \rceil$  since each user contributes  $M+K$  symbols, and the index of the corresponding code matrix as  $a-1-K-(j_a-1)(M+K)$ . Then,  $\mathbf{h}_a$ , which is the  $a$ th column of  $\mathbf{H}$ , can be written as

$$\begin{aligned} \mathbf{h}_a &= \mathbf{C}_{j_a, a-1-K-(j_a-1)(M+K)}\mathbf{g}_{j_a} \\ j_a &= \lceil a/(M+K) \rceil, \quad a = 1, \dots, L. \end{aligned} \quad (12)$$

According to (12), the signature vector of the current symbol  $w_j(n)$  for user  $j$  becomes  $\mathbf{h}_{(j-1)(M+K)+K+1}$ . For example,  $\mathbf{h}_{K+1}$  is the signature vector of  $w_1(n)$ . The structure of users' signature waveforms has been exploited to estimate all channel vectors blindly by a covariance-matching technique [17] under assumptions that all spreading codes, propagation delays, and the maximum channel delay spread are known.

### III. COVARIANCE-MATCHING CHANNEL ESTIMATION AND LINEAR DETECTION

#### A. Covariance-Matching Channel Estimation

In this subsection, we review the covariance-matching channel estimation technique proposed in [17] in order to analyze channel estimation based linear receivers later. This technique is based on the covariance of  $\mathbf{y}_n$ , which reads

$$\mathbf{R} = \sum_{j=1}^J \sum_{m=-K}^{M-1} \mathbf{C}_{j,m} \mathbf{G}_j \mathbf{C}_{j,m}^H + \sigma_v^2 \mathbf{I}_\nu \quad (13)$$

where  $\mathbf{G}_j = \sigma_{w_j}^2 \mathbf{g}_j \mathbf{g}_j^H$ . Since all input signals are drawn from the same signal constellation, without loss of generality, we may absorb the power factor of each signal into the channel vector  $\mathbf{g}_j$  and assume that all signals are transmitted at unit power  $\sigma_{w_j}^2 = 1$ . After this consideration,  $\mathbf{G}_j$  becomes  $\mathbf{g}_j \mathbf{g}_j^H$ . Correspondingly, we define  $\alpha_j = \text{tr}(\mathbf{G}_j) = \|\mathbf{g}_j\|^2$ . It is observed that  $\mathbf{R}$  is parameterized by  $\mathbf{g}_j$  in  $\mathbf{G}_j$ . If it is matched with its estimate from  $N$  data vectors

$$\hat{\mathbf{R}} = \frac{1}{N} \sum_{n=1}^N \mathbf{y}_n \mathbf{y}_n^H \quad (14)$$

and the resulting error  $\|\mathbf{R} - \hat{\mathbf{R}}\|_F^2$  is minimized,  $\mathbf{g}_j$  can be estimated. Since the cost function is highly nonlinear, minimization is performed first with respect to  $\mathbf{G}_j$  instead of  $\mathbf{g}_j$  directly. After defining  $\mathbf{r} = \text{vec}(\mathbf{R})$ ,  $\hat{\mathbf{r}} = \text{vec}(\hat{\mathbf{R}})$  and applying (1), the criterion can be described as follows [17]:

$$(\hat{\mathbf{G}}_1, \dots, \hat{\mathbf{G}}_J, \hat{\sigma}_v^2) = \arg \min_{\mathbf{G}_1, \dots, \mathbf{G}_J, \sigma_v^2} \|\mathbf{r} - \hat{\mathbf{r}}\|^2. \quad (15)$$

According to (13), we can find that

$$\mathbf{r} = \mathbf{S}\mathbf{x} \quad (16)$$

where

$$\begin{aligned} \mathbf{S} &= [\mathbf{S}_1, \dots, \mathbf{S}_J, \text{vec}(\mathbf{I}_\nu)] \\ \mathbf{S}_j &= \sum_{m=-K}^{M-1} \mathbf{C}_{j,m}^* \otimes \mathbf{C}_{j,m} \\ \mathbf{x} &= [\mathbf{x}_1^T, \dots, \mathbf{x}_J^T, \sigma_v^2]^T, \quad \mathbf{x}_j = \text{vec}(\mathbf{G}_j). \end{aligned} \quad (17)$$

Considering (16) and under some identifiability conditions [17], the solution to (15) becomes

$$\hat{\mathbf{x}} = \mathbf{Q}\hat{\mathbf{r}}, \quad \mathbf{Q} = (\mathbf{S}^H \mathbf{S})^{-1} \mathbf{S}^H \quad (18)$$

Once  $\mathbf{x}$  is estimated,  $\mathbf{x}_j$  can be extracted. Then,  $\mathbf{G}_j$  is reconstructed by the reverse vec operation. These operations can be described by

$$\begin{aligned} \hat{\mathbf{G}}_j &= [(\mathbf{e}_{q,1}^T \otimes \mathbf{I}_q) \hat{\mathbf{x}}_j, \dots, (\mathbf{e}_{q,q}^T \otimes \mathbf{I}_q) \hat{\mathbf{x}}_j] \\ \hat{\mathbf{x}}_j &= [\mathbf{e}_{j,j}^T \otimes \mathbf{I}_{q^2}, \mathbf{0}_{q^2 \times 1}] \hat{\mathbf{x}}. \end{aligned} \quad (19)$$

Using (17) and (18), we can relate  $\hat{\mathbf{G}}_j$  to  $\hat{\mathbf{r}}$

$$\hat{\mathbf{G}}_j = [\mathbf{A}_{j,1}\hat{\mathbf{r}}, \dots, \mathbf{A}_{j,q}\hat{\mathbf{r}}] \quad (20)$$

where

$$\mathbf{A}_{j,i} = (\mathbf{e}_{q,i}^T \otimes \mathbf{I}_q) [\mathbf{e}_{j,j}^T \otimes \mathbf{I}_{q^2}, \mathbf{0}_{q^2 \times 1}]_{q^2 \times (Jq^2+1)} (\mathbf{S}^H \mathbf{S})^{-1} \mathbf{S}^H$$

for  $i = 1, \dots, q$ . According to our definition of  $\mathbf{G}_j$ , if singular value decomposition is performed on this rank-one matrix, then the maximum singular value is  $\alpha_j = \|\mathbf{g}_j\|^2$ , and the corresponding singular vector becomes the channel vector up to a scalar ambiguity. The scalar ambiguity can further reduce to a phase ambiguity after considering  $\sqrt{\alpha_j}$ . Therefore, once  $\hat{\mathbf{G}}_j$  is obtained, channel vector  $\mathbf{g}_j$  can be estimated by finding the maximum singular vector of  $\hat{\mathbf{G}}_j$  and scaling the vector by  $\sqrt{\alpha_j}$  to adjust its norm. However, phase ambiguity cannot be removed by this blind technique. When estimated channel vectors are used for design of different linear receivers and, consequently, estimation of a user's input symbols, estimated symbols will incur a constant phase shift. One possible solution to tackle this problem is to transmit a few pilot symbols. In the following, we will assume that this ambiguity has been removed. Without

loss of generality, user 1 is treated as the desired user. Its symbol  $w_1(n)$  needs to be detected.

### B. Linear Detection

Linear receivers are very attractive due to their low complexity. We are particularly interested in construction of a ZF receiver, DMI MMSE receiver, subspace MMSE receiver, and RAKE receiver based on estimated channel vectors  $\hat{\mathbf{g}}_j$  and  $N$  received data vectors.

1) *ZF Receiver*: According to (10), an ideal ZF receiver can be defined as

$$\mathbf{f}_{\text{zf}} = \mathbf{H}(\mathbf{H}^H \mathbf{H})^{-1} \mathbf{e}_{L,K+1} \quad (21)$$

where  $\mathbf{e}_{L,K+1}$  is for detection of  $w_1(n)$ , whose signature vector appears in the  $(K+1)$ th column of  $\mathbf{H}$ . Once all users' channel vectors are estimated, the signature matrix  $\mathbf{H}$  can be constructed according to (11). The ZF receiver based on channel estimates becomes

$$\hat{\mathbf{f}}_{\text{zf}} = \hat{\mathbf{H}}(\hat{\mathbf{H}}^H \hat{\mathbf{H}})^{-1} \mathbf{e}_{L,K+1} \\ \hat{\mathbf{H}} = [\mathbf{C}_1(\mathbf{I}_{M+K} \otimes \hat{\mathbf{g}}_1), \dots, \mathbf{C}_J(\mathbf{I}_{M+K} \otimes \hat{\mathbf{g}}_J)]. \quad (22)$$

Then,  $w_1(n)$  is estimated by

$$\hat{w}_{1,\text{zf}}(n) = \hat{\mathbf{f}}_{\text{zf}}^H \mathbf{y}_n. \quad (23)$$

2) *DMI MMSE Receiver*: An ideal DMI MMSE receiver can be defined from direct inversion of  $\mathbf{R}$  as

$$\mathbf{f}_{\text{mmse},d} = \mathbf{R}^{-1} \mathbf{C}_{1,0} \mathbf{g}_1. \quad (24)$$

Since only finite data samples are available, the DMI MMSE receiver can be implemented as

$$\hat{\mathbf{f}}_{\text{mmse},d} = \hat{\mathbf{R}}^{-1} \mathbf{C}_{1,0} \hat{\mathbf{g}}_1 \quad (25)$$

where  $\hat{\mathbf{R}}$  is given by (14). Correspondingly, the desired symbol is estimated similarly as (23).

3) *Subspace MMSE Receiver*: The MMSE receiver can also be expressed in terms of the subspace components of  $\mathbf{R}$ . Let the eigenvalue decomposition (EVD) of  $\mathbf{R}$  be

$$\mathbf{R} = \mathbf{U}_s \mathbf{\Lambda}_s \mathbf{U}_s^H + \mathbf{U}_n \mathbf{\Lambda}_n \mathbf{U}_n^H \quad (26)$$

where  $\mathbf{U}_s$  and  $\mathbf{U}_n$  represent the signal and noise subspaces, respectively,  $\mathbf{\Lambda}_s = \text{diag}\{\lambda_1^2, \dots, \lambda_s^2\}$ ,  $\mathbf{\Lambda}_n = \sigma_v^2 \mathbf{I}$ . Invoking the orthogonality between  $\mathbf{U}_n$  and  $\mathbf{C}_{1,0} \mathbf{g}_1$ , the ideal subspace MMSE receiver takes the following form [9]:

$$\mathbf{f}_{\text{mmse},s} = \mathbf{U}_s \mathbf{\Lambda}_s^{-1} \mathbf{U}_s^H \mathbf{C}_{1,0} \mathbf{g}_1. \quad (27)$$

Then, the subspace MMSE receiver based on finite received data samples is given by

$$\hat{\mathbf{f}}_{\text{mmse},s} = \hat{\mathbf{U}}_s \hat{\mathbf{\Lambda}}_s^{-1} \hat{\mathbf{U}}_s^H \mathbf{C}_{1,0} \hat{\mathbf{g}}_1. \quad (28)$$

Similarly, the desired symbol is estimated as (23). Although the ideal subspace MMSE receiver is equivalent to the ideal DMI MMSE receiver, it is better when perturbations exist, as will be seen from our simulation results.

4) *RAKE Receiver*: An ideal RAKE receiver is constructed as

$$\mathbf{f}_{\text{rake}} = \mathbf{C}_{1,0} \mathbf{g}_1. \quad (29)$$

Based on estimated channel vector, the RAKE receiver is given by

$$\hat{\mathbf{f}}_{\text{rake}} = \mathbf{C}_{1,0} \hat{\mathbf{g}}_1 \quad (30)$$

and the desired symbol is estimated similarly as (23).

All above linear receivers are coupled with estimated channel vectors. Their performance will be investigated jointly with the channel estimator next.

## IV. PERFORMANCE ANALYSIS

In this section, performance of those linear receivers based on finite received data samples is evaluated in terms of SINR and BER. Assume that the number of data samples  $N$  is sufficiently large such that perturbation technique is applicable [20]. It will be seen that performance of the channel estimator in terms of covariance (auto-covariance, or cross-covariance, or both) is required to evaluate each receiver's performance and is thus studied first. We will derive more compact results than those in [17] based on the property of cumulant.

### A. Channel Estimation Performance

All perturbations are due to an estimation error in the data covariance  $\mathbf{R}$  or, equivalently,  $\mathbf{r}$ . From our definition of  $\mathbf{G}_j$ ,  $\mathbf{g}_j$  is the singular vector corresponding to the maximum singular value. If  $\hat{\mathbf{r}}$  has an estimation error  $\delta \mathbf{r} = \hat{\mathbf{r}} - \mathbf{r}$  due to finite  $N$ , then an error is introduced to  $\hat{\mathbf{G}}_j$ . From (20),  $\mathbf{G}_j$  is perturbed by  $\delta \mathbf{G}_j$  as

$$\delta \mathbf{G}_j = [\mathbf{A}_{j,1} \delta \mathbf{r}, \dots, \mathbf{A}_{j,q} \delta \mathbf{r}]. \quad (31)$$

Then, the first-order perturbation in its maximum singular vector becomes [20]

$$\delta \mathbf{g}_j \approx \frac{1}{\alpha_j} \mathbf{\Pi}_{\mathbf{g}_j}^\perp \delta \mathbf{G}_j \mathbf{g}_j, \quad \mathbf{\Pi}_{\mathbf{g}_j}^\perp = \mathbf{\Sigma}_j \mathbf{\Sigma}_j^H \quad (32)$$

where  $\mathbf{\Sigma}_j$  is the size of  $q \times (q-1)$  and spans a  $(q-1)$ -dimensional subspace orthogonal to  $\mathbf{g}_j$ . Substituting (31) into (32), we obtain

$$\delta \mathbf{g}_j \approx \mathbf{\Gamma}_j \delta \mathbf{r}, \quad \mathbf{\Gamma}_j = \frac{1}{\alpha_j} \mathbf{\Pi}_{\mathbf{g}_j}^\perp \sum_{i=1}^q g_j(i) \mathbf{A}_{j,i}. \quad (33)$$

Then, the auto-covariance of channel estimate becomes

$$\text{Cov}(\delta \mathbf{g}_j, \delta \mathbf{g}_j) = E \{ \delta \mathbf{g}_j \delta \mathbf{g}_j^H \} \approx \mathbf{\Gamma}_j \mathbf{\Phi}(\hat{\mathbf{r}}) \mathbf{\Gamma}_j^H \quad (34)$$

and cross-covariance between  $\delta \mathbf{g}_i$  and  $\delta \mathbf{g}_j$  is

$$\text{Cov}(\delta \mathbf{g}_i, \delta \mathbf{g}_j) = E \{ \delta \mathbf{g}_i \delta \mathbf{g}_j^H \} \approx \mathbf{\Gamma}_i \mathbf{\Phi}(\hat{\mathbf{r}}) \mathbf{\Gamma}_j^H \quad (35)$$

where  $\Phi(\hat{\mathbf{r}})$  is the covariance of  $\hat{\mathbf{r}}$

$$\Phi(\hat{\mathbf{r}}) = E\{(\hat{\mathbf{r}} - \mathbf{r})(\hat{\mathbf{r}} - \mathbf{r})^H\}. \quad (36)$$

This covariance depends on data model (10), our covariance estimation method (14), and up to the fourth-order statistics of channel inputs and noise. We present general results in the following proposition in the light of [22], which provides results for complex symmetric sources. We extend the results therein to both a real system and complex system. Although (14) does not require independence of different data vectors, we assume they are independent for convenience of analysis.

*Proposition 1:* If the channel model follows (10) with  $\nu$  outputs and  $L$  inputs that are drawn from the same signal constellation with equal probability and fourth-order cumulant  $\kappa_{4w}$ , and data covariance is estimated from  $N$  independent data vectors by (14), then for a real system, the covariance  $\Phi(\hat{\mathbf{r}})$  of  $\hat{\mathbf{r}} = \text{vec}(\hat{\mathbf{R}})$  in (36) satisfies

$$N\Phi(\hat{\mathbf{r}}) = \kappa_{4w}(\mathbf{H}\square\mathbf{H})(\mathbf{H}\square\mathbf{H})^T + \mathbf{R} \otimes \mathbf{R} + [(\mathbf{I}_\nu \otimes \mathbf{1}_\nu)\mathbf{R}(\mathbf{1}_\nu^T \otimes \mathbf{I}_\nu)] \circ [(\mathbf{1}_\nu \otimes \mathbf{I}_\nu)\mathbf{R}(\mathbf{I}_\nu \otimes \mathbf{1}_\nu^T)] \quad (37)$$

whereas for a complex system, it satisfies

$$N\Phi(\hat{\mathbf{r}}) = \kappa_{4w}(\mathbf{H}^*\square\mathbf{H})(\mathbf{H}^*\square\mathbf{H})^H + \mathbf{R}^* \otimes \mathbf{R}. \quad (38)$$

*Proof:* See Appendix A.  $\square$

This proposition shows that given the ideal data covariance  $\mathbf{R}$ , the overall channel matrix  $\mathbf{H}$ , and the fourth-order cumulant of inputs, the covariance of estimated data covariance can be obtained. Then, the channel auto-covariance  $\text{Cov}(\delta\mathbf{g}_j, \delta\mathbf{g}_j)$  can be evaluated after substituting either (37) or (38) into (34). The channel mean square error (MSE) is then the trace of  $\text{Cov}(\delta\mathbf{g}_j, \delta\mathbf{g}_j)$ . Results from (34) and (35) will be used in our analysis of different receivers. It can be observed that they are proportional to  $1/N$ .

### B. SINRs of Different Receivers

SINR is an important performance indicator for a receiver  $\mathbf{f}$ . According to (10) and (23), it can be defined as

$$\text{SINR} = \frac{\mathbf{f}^H \mathbf{R}_1 \mathbf{f}}{\mathbf{f}^H \mathbf{R}_{\text{int}} \mathbf{f}} \quad (39)$$

where  $\mathbf{R}_1 = \mathbf{C}_{1,0} \mathbf{g}_1 \mathbf{g}_1^H \mathbf{C}_{1,0}^H$ , and  $\mathbf{R}_{\text{int}} = \mathbf{R} - \mathbf{R}_1$ . Perturbation in channel estimation induced by finite data samples inevitably causes the receiver perturbed to be  $\mathbf{f} = \mathbf{f} + \delta\mathbf{f}$ , where the first-order perturbation in  $\delta\mathbf{f}$  can be assumed to have zero mean. This point will become clear after  $\delta\mathbf{f}$  is derived for each receiver up to the first order, and the zero-mean of  $\delta\mathbf{R}$  is noticed according to (14). Therefore, the perturbed SINR has the following form:

$$\widehat{\text{SINR}} = \frac{\mathbf{f}^H \mathbf{R}_1 \mathbf{f} + E\{\delta\mathbf{f}^H \mathbf{R}_1 \delta\mathbf{f}\}}{\mathbf{f}^H \mathbf{R}_{\text{int}} \mathbf{f} + E\{\delta\mathbf{f}^H \mathbf{R}_{\text{int}} \delta\mathbf{f}\}}. \quad (40)$$

This depends on both unperturbed terms (signal power, interference plus noise power) and corresponding perturbations. Pertur-

bations follow a typical form of  $\Psi(\mathbf{X}) = E\{\delta\mathbf{f}^H \mathbf{X} \delta\mathbf{f}\}$ , where  $\mathbf{X}$  can be replaced by  $\mathbf{R}_1$  or  $\mathbf{R}_{\text{int}}$ . Since different receivers take different forms with correspondingly different  $\delta\mathbf{f}$ , evaluation of  $\Psi(\mathbf{X})$  will be discussed for each receiver, respectively. For shorter notations, all receivers' subscripts are dropped later and simply denoted by  $\mathbf{f}$ . However, no confusion will be caused in the context.

1) *SINR of the ZF Receiver:* To evaluate the perturbation term, i.e.,  $\Psi(\mathbf{X})$ , we first obtain  $\delta\mathbf{f}$  according to (22). Perturbation in the signature matrix  $\mathbf{H}$  is given by

$$\begin{aligned} \delta\mathbf{H} &= [\delta\mathbf{h}_1, \dots, \delta\mathbf{h}_L] \\ &= [\mathbf{C}_1(\mathbf{I}_{M+K} \otimes \delta\mathbf{g}_1), \dots, \mathbf{C}_J(\mathbf{I}_{M+K} \otimes \delta\mathbf{g}_J)] \end{aligned} \quad (41)$$

according to (22). Similar to (12), the  $a$ th column of  $\delta\mathbf{H}$  can be written as

$$\begin{aligned} \delta\mathbf{h}_a &= \mathbf{C}_{j_a, a-1-K-(j_a-1)(M+K)} \delta\mathbf{g}_{j_a} \\ j_a &= \lceil a/(M+K) \rceil, \quad a = 1, \dots, L. \end{aligned} \quad (42)$$

Noticing  $\hat{\mathbf{H}} = \mathbf{H} + \delta\mathbf{H}$ , expanding  $(\hat{\mathbf{H}}^H \hat{\mathbf{H}})^{-1}$  into a Taylor series, and keeping only the first-order terms, we obtain

$$\begin{aligned} \delta\mathbf{f} &\approx \mathbf{\Pi}_H^\perp \delta\mathbf{H}(\mathbf{H}^H \mathbf{H})^{-1} \mathbf{e}_{L, K+1} \\ &\quad - (\mathbf{H}^\dagger)^H \delta\mathbf{H} \mathbf{H} (\mathbf{H}^\dagger)^H \mathbf{e}_{L, K+1} \end{aligned} \quad (43)$$

where  $\mathbf{\Pi}_H^\perp = \mathbf{I}_\nu - \mathbf{H} \mathbf{H}^\dagger$ , and  $\mathbf{H}^\dagger = (\mathbf{H}^H \mathbf{H})^{-1} \mathbf{H}^H$ . Then

$$\begin{aligned} \Psi(\mathbf{X}) &\approx \mathbf{e}_{L, K+1}^H (\mathbf{H}^H \mathbf{H})^{-1} \underline{E\{\delta\mathbf{H}^H \mathbf{\Pi}_H^\perp \mathbf{X} \mathbf{\Pi}_H^\perp \delta\mathbf{H}\}} \\ &\quad \times (\mathbf{H}^H \mathbf{H})^{-1} \mathbf{e}_{L, K+1} \\ &\quad - \mathbf{e}_{L, K+1}^H (\mathbf{H}^H \mathbf{H})^{-1} \underline{E\{\delta\mathbf{H}^H \mathbf{\Pi}_H^\perp \mathbf{X} (\mathbf{H}^\dagger)^H \delta\mathbf{H}\}} \\ &\quad \times (\mathbf{H}^\dagger)^H \mathbf{e}_{L, K+1} \\ &\quad - \mathbf{e}_{L, K+1}^H \mathbf{H}^\dagger \underline{E\{\delta\mathbf{H} \mathbf{H}^\dagger \mathbf{X} \mathbf{\Pi}_H^\perp \delta\mathbf{H}\}} \\ &\quad \times (\mathbf{H}^H \mathbf{H})^{-1} \mathbf{e}_{L, K+1} \\ &\quad + \mathbf{e}_{L, K+1}^H \mathbf{H}^\dagger \underline{E\{\delta\mathbf{H} \mathbf{H}^\dagger \mathbf{X} (\mathbf{H}^\dagger)^H \delta\mathbf{H}\}} \\ &\quad \times (\mathbf{H}^\dagger)^H \mathbf{e}_{L, K+1}. \end{aligned} \quad (44)$$

It can be found that those underlined terms follow forms of  $E\{\delta\mathbf{H} \mathbf{Z} \delta\mathbf{H}^H\}$ ,  $E\{\delta\mathbf{H}^H \mathbf{Z} \delta\mathbf{H}\}$ ,  $E\{\delta\mathbf{H} \mathbf{Z} \delta\mathbf{H}\}$ ,  $E\{\delta\mathbf{H}^H \mathbf{Z} \delta\mathbf{H}^H\}$ , where  $\mathbf{Z}$  is replaced by corresponding deterministic quantities. The last form can be obtained after Hermitian operation on the third form. Therefore, we only need to simplify the first three forms. Each of them requires statistics  $E\{\delta\mathbf{h}_a \delta\mathbf{h}_b^H\}$  for  $a, b = 1, \dots, L$ . According to (42), we have

$$\begin{aligned} E\{\delta\mathbf{h}_a \delta\mathbf{h}_b^H\} &= \mathbf{C}_{j_a, a-1-K-(j_a-1)(M+K)} E\{\delta\mathbf{g}_{j_a} \delta\mathbf{g}_{j_b}^H\} \\ &\quad \times \mathbf{C}_{j_b, b-1-K-(j_b-1)(M+K)}^H \end{aligned} \quad (45)$$

where

$$\begin{aligned} j_a &= \lceil a/(M+K) \rceil, \quad j_b = \lceil b/(M+K) \rceil \\ a, b &= 1, \dots, L \end{aligned} \quad (46)$$

and  $E\{\delta\mathbf{g}_{j_a} \delta\mathbf{g}_{j_b}^H\}$  can be obtained from either (34) if  $j_a = j_b$  or (35) if  $j_a \neq j_b$ . Detailed derivations of these three typical terms are provided in Appendix B.

2) *SINR of the DMI MMSE Receiver*: The DMI MMSE receiver is given by (25). Expressing  $\hat{\mathbf{R}}$  as  $\mathbf{R} + \delta\mathbf{R}$  and performing Taylor's expansion

$$(\mathbf{R} + \delta\mathbf{R})^{-1} \approx \mathbf{R}^{-1} - \mathbf{R}^{-1}\delta\mathbf{R}\mathbf{R}^{-1} \quad (47)$$

we obtain the first-order perturbation of the receiver

$$\delta\mathbf{f} \approx \mathbf{R}^{-1}\mathbf{C}_{1,0}\delta\mathbf{g}_1 - \mathbf{R}^{-1}\delta\mathbf{R}\mathbf{R}^{-1}\mathbf{C}_{1,0}\mathbf{g}_1. \quad (48)$$

Substituting (33) into (48),  $\delta\mathbf{f}$  is related to perturbation in covariance estimation in both vector form  $\delta\mathbf{r}$  and matrix form  $\delta\mathbf{R}$  by

$$\delta\mathbf{f} \approx \mathbf{R}^{-1}\mathbf{C}_{1,0}\mathbf{\Gamma}_1\delta\mathbf{r} - \mathbf{R}^{-1}\delta\mathbf{R}\mathbf{R}^{-1}\mathbf{C}_{1,0}\mathbf{g}_1. \quad (49)$$

Based on (49), perturbation of signal/noise power  $\Psi(\mathbf{X})$  is given by

$$\begin{aligned} \Psi(\mathbf{X}) \approx & \text{tr} \left( \underline{E\{\delta\mathbf{r}\delta\mathbf{r}^H\}}\mathbf{\Gamma}_1^H \underline{\mathbf{C}_{1,0}^H \mathbf{R}^{-1} \mathbf{X} \mathbf{R}^{-1} \mathbf{C}_{1,0} \mathbf{\Gamma}_1} \right) \\ & + \underline{\mathbf{g}_1^H \mathbf{C}_{1,0}^H \mathbf{R}^{-1} E\{\delta\mathbf{R}\mathbf{R}^{-1} \mathbf{X} \mathbf{R}^{-1} \delta\mathbf{R}\} \mathbf{R}^{-1} \mathbf{C}_{1,0} \mathbf{g}_1} \\ & - \underline{\mathbf{g}_1^H \mathbf{C}_{1,0}^H \mathbf{R}^{-1} E\{\delta\mathbf{R}\mathbf{R}^{-1} \mathbf{X} \mathbf{R}^{-1} \mathbf{C}_{1,0} \mathbf{\Gamma}_1 \delta\mathbf{r}\}} \\ & - \underline{E\{\delta\mathbf{r}^H \mathbf{\Gamma}_1^H \mathbf{C}_{1,0}^H \mathbf{R}^{-1} \mathbf{X} \mathbf{R}^{-1} \delta\mathbf{R}\} \mathbf{R}^{-1} \mathbf{C}_{1,0} \mathbf{g}_1}. \end{aligned} \quad (50)$$

Those underlined terms are required for evaluation of  $\Psi(\mathbf{X})$ . The first term can be easily obtained after results from Proposition 1 are applied. The second term has been derived in [21] in a general form  $E\{\delta\mathbf{R}\mathbf{Z}\delta\mathbf{R}\}$ , where  $\mathbf{Z}$  is an arbitrary deterministic matrix. For clarity, we restate the results in the following proposition.

*Proposition 2 [21]*: If the channel model follows (10) with  $L$  inputs and  $\nu$  outputs and data covariance is estimated from  $N$  independent data vectors by (14), then for a real system, the covariance of  $\delta\mathbf{R}$  weighted by a constant matrix  $\mathbf{Z}$  satisfies

$$\begin{aligned} NE\{\delta\mathbf{R}\mathbf{Z}\delta\mathbf{R}\} = & \kappa_{4w}\mathbf{H}[\mathbf{I}_L \odot (\mathbf{H}^T \mathbf{Z} \mathbf{H})] \mathbf{H}^T \\ & + \text{tr}(\mathbf{R}\mathbf{Z})\mathbf{R} + \mathbf{R}\mathbf{Z}^T \mathbf{R} \end{aligned} \quad (51)$$

and for a complex system, it satisfies

$$NE\{\delta\mathbf{R}\mathbf{Z}\delta\mathbf{R}\} = \kappa_{4w}\mathbf{H}[\mathbf{I}_L \odot (\mathbf{H}^H \mathbf{Z} \mathbf{H})] \mathbf{H}^H + \text{tr}(\mathbf{R}\mathbf{Z})\mathbf{R}. \quad (52)$$

□

Replacing  $\mathbf{Z}$  by  $\mathbf{R}^{-1}\mathbf{X}\mathbf{R}^{-1}$ , the second underlined term in (50) follows. The third and fourth underlined terms  $E\{\delta\mathbf{R}\mathbf{Z}\delta\mathbf{r}\}$  and  $E\{\delta\mathbf{r}^H \mathbf{Z} \delta\mathbf{R}\}$  are simplified in Appendix C, where  $\mathbf{Z}$  can be substituted by corresponding quantities  $\mathbf{R}^{-1}\mathbf{X}\mathbf{R}^{-1}\mathbf{C}_{1,0}\mathbf{\Gamma}_1$  and  $\mathbf{\Gamma}_1^H \mathbf{C}_{1,0}^H \mathbf{R}^{-1} \mathbf{X} \mathbf{R}^{-1}$ , respectively.

3) *SINR of the Subspace MMSE Receiver*: According to (28) and expanding  $(\mathbf{\Lambda}_s + \delta\mathbf{\Lambda}_s)^{-1}$ , we obtain

$$\begin{aligned} \delta\mathbf{f} \approx & \delta\mathbf{U}_s \mathbf{\Lambda}_s^{-1} \mathbf{U}_s^H \mathbf{C}_{1,0} \mathbf{g}_1 - \mathbf{U}_s \mathbf{\Lambda}_s^{-1} \delta\mathbf{\Lambda}_s \mathbf{\Lambda}_s^{-1} \mathbf{U}_s^H \mathbf{C}_{1,0} \mathbf{g}_1 \\ & + \mathbf{U}_s \mathbf{\Lambda}_s^{-1} \delta\mathbf{U}_s^H \mathbf{C}_{1,0} \mathbf{g}_1 + \mathbf{U}_s \mathbf{\Lambda}_s^{-1} \mathbf{U}_s^H \mathbf{C}_{1,0} \delta\mathbf{g}_1. \end{aligned} \quad (53)$$

Perturbation  $\delta\mathbf{R}$  or  $\delta\mathbf{r}$  causes not only the estimated channel vector being perturbed but the subspace components of  $\mathbf{R}$  to be perturbed as well. The results can be found in the following.

*Proposition 3 [20]*: If  $\mathbf{R}$  is perturbed by  $\delta\mathbf{R}$ , then its eigen-components are perturbed by

$$\begin{aligned} \delta\mathbf{U}_s & \approx \mathbf{U}_n \mathbf{U}_n^H \delta\mathbf{R} \mathbf{U}_s \mathbf{\Omega}^{-1}, \delta\mathbf{U}_n \approx -\mathbf{U}_s \mathbf{\Omega}^{-1} \mathbf{U}_s^H \delta\mathbf{R} \mathbf{U}_n \\ \delta\mathbf{\Lambda}_s & \approx \mathbf{U}_s^H \delta\mathbf{R} \mathbf{U}_s, \delta\mathbf{\Lambda}_n \approx \mathbf{U}_n^H \delta\mathbf{R} \mathbf{U}_n \end{aligned} \quad (54)$$

where

$$\mathbf{\Omega} = \mathbf{\Lambda}_s - \sigma_v^2 \mathbf{I}$$

and approximation is valid up to the first order of  $\delta\mathbf{R}$ . □

Since  $\mathbf{U}_n^H \mathbf{C}_{1,0} \mathbf{g}_1 = \mathbf{0}$ , by substituting (54) in (53) and invoking (33), we obtain

$$\delta\mathbf{f} \approx \mathbf{B}_n \delta\mathbf{R} \mathbf{B}_\gamma \mathbf{C}_{1,0} \mathbf{g}_1 - \mathbf{B}_s \delta\mathbf{R} \mathbf{B}_s \mathbf{C}_{1,0} \mathbf{g}_1 + \mathbf{B}_s \mathbf{C}_{1,0} \mathbf{\Gamma}_1 \delta\mathbf{r} \quad (55)$$

where, for convenience, we have defined

$$\mathbf{B}_n \triangleq \mathbf{U}_n \mathbf{U}_n^H, \mathbf{B}_s \triangleq \mathbf{U}_s \mathbf{\Lambda}_s^{-1} \mathbf{U}_s^H, \mathbf{B}_\gamma \triangleq \mathbf{U}_s (\mathbf{\Omega} \mathbf{\Lambda}_s)^{-1} \mathbf{U}_s^H.$$

Then,  $\Psi(\mathbf{X})$  can be expressed in terms of statistics of the covariance estimation error

$$\begin{aligned} \Psi(\mathbf{X}) \approx & \mathbf{g}_1^H \mathbf{C}_{1,0}^H \mathbf{B}_\gamma E\{\delta\mathbf{R} \mathbf{B}_n \mathbf{X} \mathbf{B}_n \delta\mathbf{R}\} \mathbf{B}_\gamma \mathbf{C}_{1,0} \mathbf{g}_1 \\ & - \mathbf{g}_1^H \mathbf{C}_{1,0}^H \mathbf{B}_\gamma E\{\delta\mathbf{R} \mathbf{B}_n \mathbf{X} \mathbf{B}_s \delta\mathbf{R}\} \mathbf{B}_s \mathbf{C}_{1,0} \mathbf{g}_1 \\ & + \mathbf{g}_1^H \mathbf{C}_{1,0}^H \mathbf{B}_\gamma E\{\delta\mathbf{R} \mathbf{B}_n \mathbf{X} \mathbf{B}_s \mathbf{C}_{1,0} \mathbf{\Gamma}_1 \delta\mathbf{r}\} \\ & - \mathbf{g}_1^H \mathbf{C}_{1,0}^H \mathbf{B}_s E\{\delta\mathbf{R} \mathbf{B}_s \mathbf{X} \mathbf{B}_n \delta\mathbf{R}\} \mathbf{B}_\gamma \mathbf{C}_{1,0} \mathbf{g}_1 \\ & + \mathbf{g}_1^H \mathbf{C}_{1,0}^H \mathbf{B}_s E\{\delta\mathbf{R} \mathbf{B}_s \mathbf{X} \mathbf{B}_s \delta\mathbf{R}\} \mathbf{B}_s \mathbf{C}_{1,0} \mathbf{g}_1 \\ & - \mathbf{g}_1^H \mathbf{C}_{1,0}^H \mathbf{B}_s E\{\delta\mathbf{R} \mathbf{B}_s \mathbf{X} \mathbf{B}_s \mathbf{C}_{1,0} \mathbf{\Gamma}_1 \delta\mathbf{r}\} \\ & + \underline{E\{\delta\mathbf{r}^H \mathbf{\Gamma}_1^H \mathbf{C}_{1,0}^H \mathbf{B}_s \mathbf{X} \mathbf{B}_n \delta\mathbf{R}\} \mathbf{B}_\gamma \mathbf{C}_{1,0} \mathbf{g}_1} \\ & - \underline{E\{\delta\mathbf{r}^H \mathbf{\Gamma}_1^H \mathbf{C}_{1,0}^H \mathbf{B}_s \mathbf{X} \mathbf{B}_s \delta\mathbf{R}\} \mathbf{B}_s \mathbf{C}_{1,0} \mathbf{g}_1} \\ & + \text{tr} \left( \underline{E\{\delta\mathbf{r}\delta\mathbf{r}^H\}}\mathbf{\Gamma}_1^H \mathbf{C}_{1,0}^H \mathbf{B}_s \mathbf{X} \mathbf{B}_s \mathbf{C}_{1,0} \mathbf{\Gamma}_1 \right). \end{aligned} \quad (56)$$

Each underlined term in (56) can be evaluated according to either Proposition 1, Proposition 2, or Appendix C, respectively. The first, second, fourth, and fifth terms are obtained from Proposition 2. The third, sixth, seventh, and eighth terms are obtained from Appendix C. The last term is obtained from Proposition 1.

4) *SINR of the RAKE Receiver*: According to (30), we obtain

$$\delta\mathbf{f} = \mathbf{C}_{1,0} \delta\mathbf{g}_1. \quad (57)$$

Then, perturbation of the signal/noise power  $\Psi(\mathbf{X})$  is given by

$$\begin{aligned} \Psi(\mathbf{X}) & = E\{\delta\mathbf{g}_1^H \mathbf{C}_{1,0}^H \mathbf{X} \mathbf{C}_{1,0} \delta\mathbf{g}_1\} \\ & = \text{tr} \left( \underline{E\{\delta\mathbf{g}_1 \delta\mathbf{g}_1^H\}} \mathbf{C}_{1,0}^H \mathbf{X} \mathbf{C}_{1,0} \right) \end{aligned} \quad (58)$$

where  $E\{\delta\mathbf{g}_1 \delta\mathbf{g}_1^H\}$  can be obtained from (34).

### C. BER Performance of Different Receivers

For each receiver, once its output SINR is evaluated, BER can be obtained by assuming that the interference is Gaussian distributed. This may not be accurate, but this approximation has been shown to be relatively good [25], [26], especially when the number of interfering symbols is large. The BER for BPSK information symbol is

$$\widehat{\text{BER}} = Q(\sqrt{\widehat{\text{SINR}}}) \quad (59)$$

where  $Q(x) = (1/\sqrt{2\pi}) \int_x^\infty e^{-(t^2)/2} dt$ . Approximated BERs will be compared with corresponding experimental ones by simulation examples.

## V. SIMULATION EXAMPLES

We verify analytical results by computer simulation. Since channel estimation MSEs have been well studied in [17], we only show performance of the following receivers based on finite received data samples and estimated channel parameters: ZF, DMI MMSE, subspace MMSE, and RAKE receivers. The average SINR and BER of each receiver over 100 independent realizations are used as performance measures. Experimental SINRs and BERs are compared with analytical ones. Except being stated otherwise, we assume eight equal-power users in a CDMA system. Users' BPSK data symbols are spread by different Gold sequences of length 31. Channel coefficients for each user are selected from a randomly generated Gaussian process with zero mean and unit variance. Then, each channel vector is normalized. The maximum channel delay spread is assumed to be five chips. The SNR is set to be 10 dB, and  $M$  is set to be 1. One user is treated as the desired user. Effects of the sample size  $N$ , SNR, near-far situation, and number of users are studied as follows.

### A. Effects of $N$

Finite  $N$  causes errors in channel estimation and symbol detection. Channel estimation errors introduce errors to different linear receivers constructed from estimated channel parameters. Fig. 1 presents SINRs versus  $N$  over a large range from  $10^2$  to  $10^4$  for a ZF receiver, DMI MMSE receiver, subspace MMSE receiver, and RAKE receiver in subplots (a)–(d), respectively. Dashed-dotted lines are based on ideal receivers that do not depend on  $N$  [see (21), (24), (27), and (29)], dashed lines represent analytical results obtained according to (40), and solid lines stand for experimental results based on finite received data samples [see (22), (25), (28), and (30)]. It is clearly seen that dashed line and solid line agree with each other in each subplot even for relatively small  $N$ . It indicates that analytical results based on a large  $N$  assumption can still reliably predict both the channel estimator's and receivers' performance with a finite number of samples. Convergence of both dashed and solid lines to the dashed-dotted line in each subplot for sufficiently large  $N$  is also observed. The ZF receiver utilizes estimated channel vectors for all users, whereas all other receivers require only the estimated channel vector for the desired user. Performance of the ZF receiver is not very sensitive to  $N$ , mainly due to relatively satisfactory channel estimation performance at small  $N$

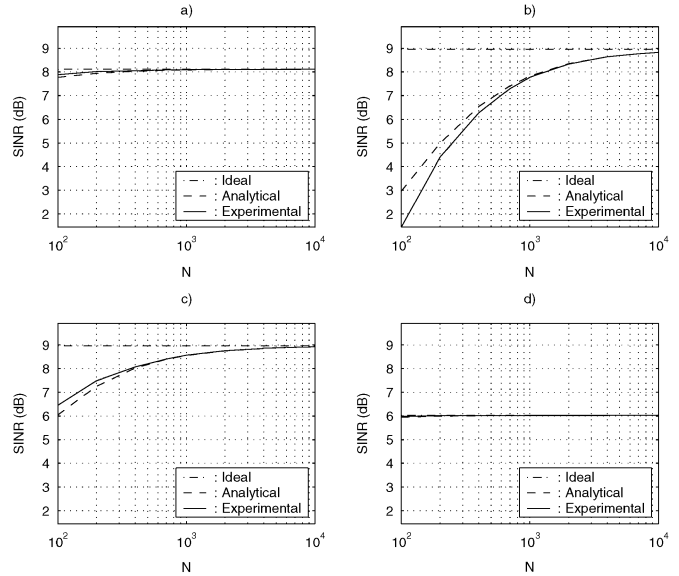


Fig. 1. SINRs of different receivers versus  $N$ . (a) ZF. (b) DMI MMSE. (c) Subspace MMSE. (d) RAKE.

[17]. On the contrary, the SINR of the DMI MMSE receiver (25) depends heavily on  $N$ , starting from about 2 dB and ending at 9 dB. It is sensitive to the inversion of the estimation error in the data covariance because of the inversion of the data covariance matrix. Compared with the subspace MMSE receiver (28), it has an additional term  $\hat{U}_n \hat{\Lambda}_n^{-1} \hat{U}_n^H \mathbf{C}_{1,0} \hat{\mathbf{g}}_1$  after  $\hat{\mathbf{R}}$  is substituted by its subspace decomposition form. This term causes a large error for high SNR because of  $\hat{\Lambda}_n^{-1}$  and nonorthogonality of the estimated signature waveform  $\mathbf{C}_{1,0} \hat{\mathbf{g}}_1$  to the estimated noise subspace  $\hat{U}_n$ . In the current setup with SNR = 10 dB,  $\hat{\Lambda}_n^{-1}$  makes a significant difference from the subspace MMSE receiver and yields slower convergence for the DMI MMSE receiver. For moderate  $N$  such as  $N = 500$ , the difference is as large as 1.5 dB (about 6.5 dB versus 8 dB). At small  $N$ , the subspace MMSE receiver provides a much higher SINR than the DMI MMSE receiver. Thus, for finite  $N$ , the subspace MMSE receiver performs much better than the DMI MMSE receiver. This will also be verified by results presented later. However, as  $N$  increases, covariance estimation becomes more reliable, leading to more accurate estimates of noise subspace and channel. As a consequence, that additional term makes less of a contribution with increased  $N$  and even disappears as  $N \rightarrow \infty$ . Both MMSE receivers yield the same convergence SINR level for large  $N$ , as expected. The gap between the solid line and dashed line tends to diminish at large  $N$  for all receivers including ZF and RAKE receivers. The convergence level of two MMSE receivers is higher than that of the ZF receiver. The RAKE receiver does not show performance improvement as  $N$  increases. Differences in SINRs can be reflected in BERs presented in Fig. 2. Dashed lines are obtained from (59) using analytical SINRs in the previous figure. Dashed-dotted lines and solid lines are obtained from simulations. It is clear that each solid line converges to the corresponding dashed line, indicating that the interference plus noise can be reasonably modeled as a Gaussian random process [25], [26]. BERs for two MMSE receivers decay with  $N$ , whereas for other receivers, they remain almost unchanged,

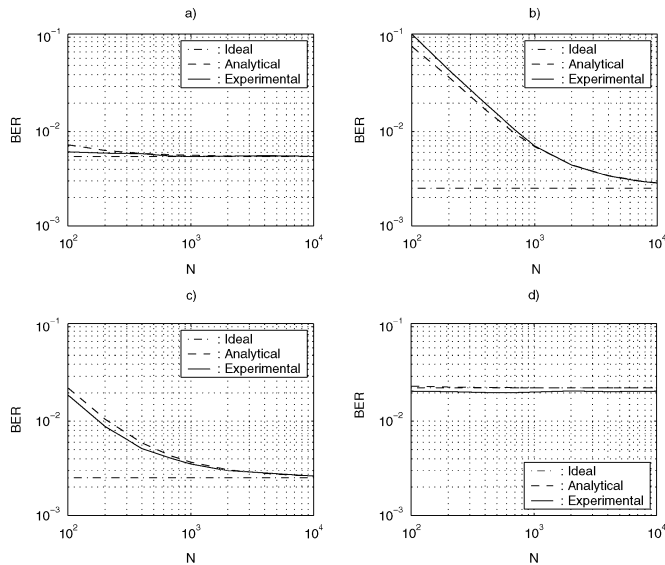


Fig. 2. BERs of different RAKE receivers versus  $N$ . (a) ZF. (b) DMI MMSE. (c) Subspace MMSE. (d) RAKE.

which is consistent with SINR results. Again, BER convergence of receivers to that of the ideal receivers is observed for large  $N$ .

### B. Effects of SNR

In this experiment, effects of SNR from 0 to 20 dB at a 2-dB interval on the receivers' performance are tested when channel vectors are estimated based on  $N = 500$  data vectors. Corresponding results are presented in Figs. 3 and 4. The SINR performance changes differently for different receivers, as seen from Fig. 3. The ZF receiver gives the best SINR at high SNRs. It is interesting to see that the DMI MMSE receiver based on finite received data samples does not improve with increased SNR monotonically. In addition, the error between the analytical and experimental results turns out to be larger. The subspace MMSE receiver behaves almost as satisfactorily as the ZF receiver with slight degradation at high SNRs, although only the desired user's channel vector is required. The RAKE receiver performs closely to the DMI MMSE receiver in this case. The performance difference between the ideal MMSE receiver and channel estimation-based DMI MMSE receiver for finite  $N$  and at high SNR has been previously explained. It depends on both  $N$  and SNR. At low SNR,  $N$  is an important factor that affects the performance, whereas at high SNR, noise becomes a dominant factor. This transition can be observed from non-monotony of the dashed and solid lines in Fig. 3(b). The SINR peak happens to be around SNR = 15 dB. The gap between the dashed-dotted line and other lines for two MMSE receivers are due to finite  $N$  (currently 500). BERs of all receivers are plotted in Fig. 4. For SNRs higher than 15 dB, the BERs for the ZF and subspace MMSE receivers lie below  $10^{-4}$ . Experimental results for these two receivers converge to the corresponding analytical results. The DMI MMSE and RAKE receivers perform much worse, especially at high SNRs. The analytical results deviate from the experimental ones at high SNRs, which is significant for the DMI MMSE receiver. The reason, for the DMI MMSE

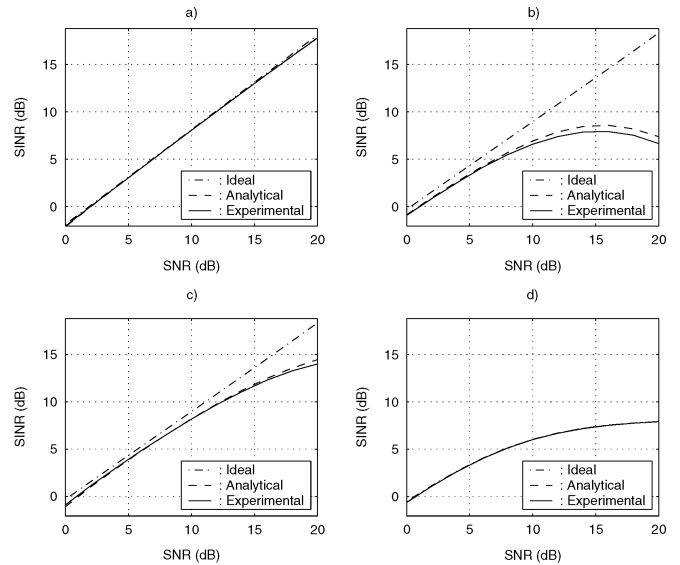


Fig. 3. SINRs of different RAKE receivers versus SNR. (a) ZF. (b) DMI MMSE. (c) Subspace MMSE. (d) RAKE.

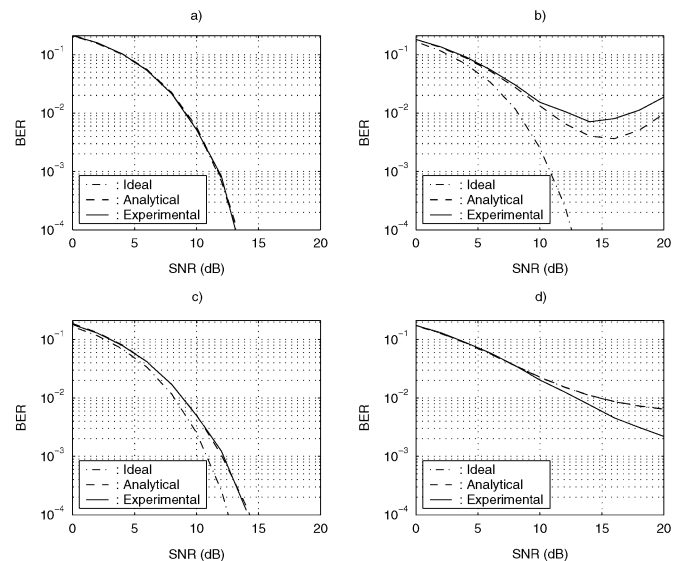


Fig. 4. BERs of different receivers versus SNR. (a) ZF. (b) DMI MMSE. (c) Subspace MMSE. (d) RAKE.

receiver, is its sensitivity to covariance estimation error with finite  $N$ , and the reason for the RAKE receiver is the possible violation of the Gaussian assumption for the interference plus noise at high SNRs.

In order to better show the sensitivity of both MMSE receivers to SNR and sample size  $N$ , we further test SINRs and BERs versus SNR for different  $N$ . Corresponding results are plotted in Fig. 5. Fig. 5(a) and (b) are for the SINRs of the DMI and subspace MMSE receivers, respectively, whereas Fig. 5(c) and (d) are their BERs. The dashed line in each subplot represents performance of the ideal MMSE receiver associated with  $N = \infty$ , whereas the other six solid lines show results for  $N = 50, 150, 300, 500, 1000,$  and  $2000$ , respectively. Although only marks  $N = 50$  and  $N = 150$  are provided for clean plots, lines are shown for different  $N$  successively in that order from bottom to top in Fig. 5(a) and (b) and from top to bottom in Fig. 5(c) and

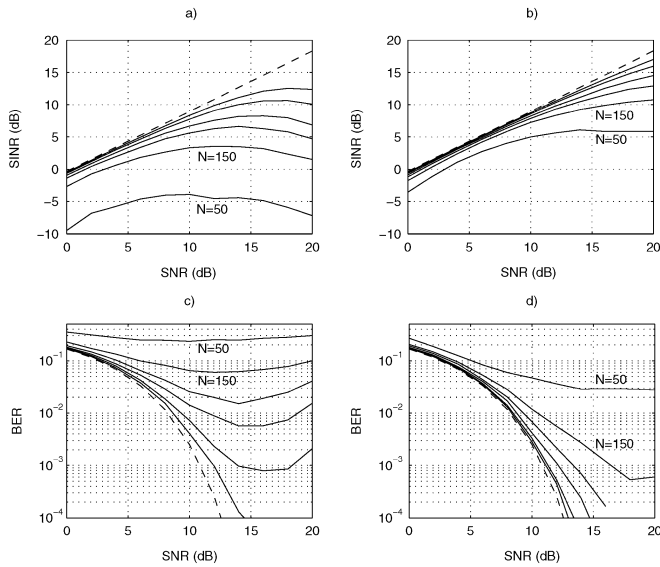


Fig. 5. Effects of SNR and  $N$  ( $N$  takes values 50, 150, 300, 500, 1000, 2000, and  $\infty$  successively). (a) DMI MMSE. (b) Subspace MMSE. (c) DMI MMSE. (d) Subspace MMSE.

(d). The SINR peaks for the DMI MMSE receiver are clearly observed for small to moderate  $N$ . They shift to high SNR regions as  $N$  increases. Meanwhile, the right-hand side of each line decreases more slowly. As  $N \rightarrow \infty$ , peak disappears, and the solid line converges to the dashed one. However, the SINR of the subspace MMSE receiver almost shows no peak for all  $N$ . It converges to the ideal one much faster than that of the DMI MMSE receiver. Similar conclusions can be made from BER results. Compared with the ideal MMSE receiver, performance degradation of two channel estimation-based MMSE receivers always occurs due to finite data sample-induced estimation error, although the subspace MMSE receiver performs much better than the DMI MMSE receiver in many cases. Not surprisingly, this is also applicable for results presented later. Due to the same reason, a detailed explanation will be omitted.

C. Near-Far Effects

To test near-far effects, we fix the SNR level while varying the signal-to-interference ratio (SIR) from  $-10$  to  $10$  dB. The SIR is defined from the desired signal power and the power of one of the other seven equal power interfering users. Fig. 6 plots the SINRs. Consistency between analytical and experimental results can be observed. The ZF and subspace MMSE receivers are much less sensitive to SIRs than the other two receivers. The RAKE receiver relies more heavily on the desired signal power than the DMI MMSE receiver.

D. Effects of Number of Users

The ability of a receiver to combat MUI is desirable. The number of users directly affects the total interference level. We thus test the sensitivity of different receivers, and let the number of users  $J$  vary from 2 to 20 by increments of 2 at each step. Fig. 7 shows the SINR performance. Up to 20 users, the first three receivers yield similar SINRs. The SINR for each of them decreases at a constant slope. The SINR of the RAKE receiver

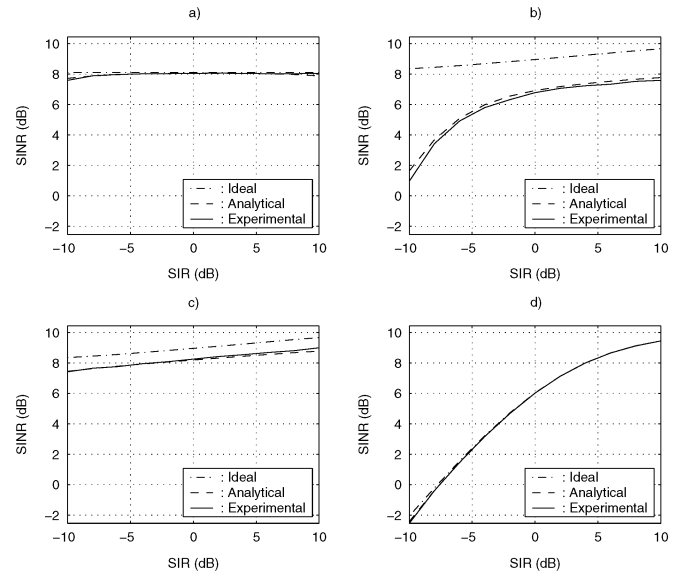


Fig. 6. SINRs of different receivers versus SIR. (a) ZF. (b) DMI MMSE. (c) Subspace MMSE. (d) RAKE.

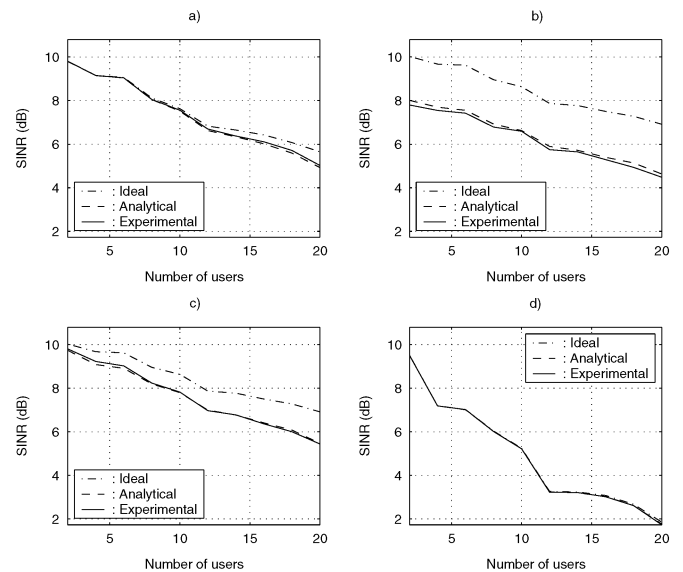


Fig. 7. SINRs of different receivers versus number of users. (a) ZF. (b) DMI MMSE. (c) Subspace MMSE. (d) RAKE.

decays much faster since as  $J$  increases, this receiver is unable to mitigate significant interference introduced to the system.

VI. CONCLUSION

This paper analyzes different linear receivers from a perturbation perspective when channel parameters are not perfectly estimated by a blind method due to finite received data samples. Experimental results are consistent with analytical ones in many examined situations. As byproducts, statistics of vectored sample covariance are derived. Meanwhile, weighted covariance between the sample covariance matrix and vectored sample covariance is provided. Those results can be applied to analyze other covariance-based algorithms as well whenever appropriate, similar to existing statistical results for the weighted sample covariance matrix.

APPENDIX A  
PROOF OF PROPOSITION 1

For convenience, define  $\hat{\mathbf{r}}_n = \text{vec}(\mathbf{y}_n \mathbf{y}_n^H)$  as the instantaneous vectored covariance. Then, it can be easily verified that the covariance of  $\hat{\mathbf{r}}$  has a form

$$\begin{aligned} \Phi(\hat{\mathbf{r}}) &= E\{(\hat{\mathbf{r}} - \mathbf{r})(\hat{\mathbf{r}} - \mathbf{r})^H\} \\ &= \frac{1}{N^2} \sum_{n_1, n_2=1}^N E\{\hat{\mathbf{r}}_{n_1} \hat{\mathbf{r}}_{n_2}^H\} - \mathbf{r} \mathbf{r}^H \end{aligned} \quad (60)$$

where we have used  $E\{\hat{\mathbf{r}}_{n_1}\} = E\{\hat{\mathbf{r}}_{n_2}\} = \mathbf{r}$ . Considering all possible values that  $n_1$  and  $n_2$  take, the summation can be expanded into  $n_1 = n_2$  and  $n_1 \neq n_2$ . The latter gives  $(1)/(N^2)(N^2 - N)\mathbf{r}\mathbf{r}^H$  due to our independence assumption of data vectors used for covariance estimation. Together with the result from the first, (60) becomes

$$N\Phi(\hat{\mathbf{r}}) = E\{\hat{\mathbf{r}}_n \hat{\mathbf{r}}_n^H\} - \mathbf{r} \mathbf{r}^H. \quad (61)$$

Expressing  $\hat{\mathbf{r}}_n$  as  $\mathbf{y}_n^* \otimes \mathbf{y}_n$  according to (2), (61) becomes

$$N\Phi(\hat{\mathbf{r}}) = E\{(\mathbf{y}_n^* \otimes \mathbf{y}_n)(\mathbf{y}_n^* \otimes \mathbf{y}_n)^H\} - \mathbf{r} \mathbf{r}^H. \quad (62)$$

It is necessary to simplify a key term  $E\{(\mathbf{y}_n^* \otimes \mathbf{y}_n)(\mathbf{y}_n^* \otimes \mathbf{y}_n)^H\}$  in (62). Some results have been derived for complex variables  $\mathbf{y}_n$  in [22]. We will complete derivation for real variables and reiterate results for complex variables as well for integrity.

Denote elements of  $\mathbf{y}_n$  by  $y_i$  for  $i = 1, \dots, \nu$ . For a zero mean vector  $\mathbf{y}_n$ , define the fourth-order cumulant matrix as [22]

$$\mathbf{K}_y = \sum_{a,b,c,d=1}^{\nu} (\mathbf{e}_{\nu,b} \otimes \mathbf{e}_{\nu,a})(\mathbf{e}_{\nu,c} \otimes \mathbf{e}_{\nu,d})^T \text{cum}(y_a, y_b^*, y_c, y_d^*)$$

where

$$\begin{aligned} \text{cum}(y_a, y_b^*, y_c, y_d^*) &= E\{y_a y_b^* y_c y_d^*\} - E\{y_a y_b^*\} E\{y_c y_d^*\} \\ &\quad - E\{y_a y_d^*\} E\{y_b^* y_c\} \\ &\quad - E\{y_a y_c\} E\{y_b^* y_d^*\}. \end{aligned}$$

It can be written compactly as [22]

$$\begin{aligned} \mathbf{K}_y &= E\{(\mathbf{y}_n^* \otimes \mathbf{y}_n)(\mathbf{y}_n^T \otimes \mathbf{y}_n^H)\} \\ &\quad - E\{\mathbf{y}_n^* \otimes \mathbf{y}_n\} E\{\mathbf{y}_n^T \otimes \mathbf{y}_n^H\} \\ &\quad - E\{\mathbf{y}_n^* \mathbf{y}_n^T\} \otimes E\{\mathbf{y}_n \mathbf{y}_n^H\} \\ &\quad - E\{(\mathbf{y}_n^* \otimes \mathbf{1}_\nu)(\mathbf{1}_\nu \otimes \mathbf{y}_n)^H\} \\ &\quad \odot E\{(\mathbf{1}_\nu \otimes \mathbf{y}_n)(\mathbf{y}_n^* \otimes \mathbf{1}_\nu)^H\} \end{aligned} \quad (63)$$

from which we obtain

$$\begin{aligned} E\{(\mathbf{y}_n^* \otimes \mathbf{y}_n)(\mathbf{y}_n^T \otimes \mathbf{y}_n^H)\} &= \mathbf{K}_y + E\{\mathbf{y}_n^* \otimes \mathbf{y}_n\} E\{\mathbf{y}_n^T \otimes \mathbf{y}_n^H\} \\ &\quad + E\{\mathbf{y}_n^* \mathbf{y}_n^T\} \otimes E\{\mathbf{y}_n \mathbf{y}_n^H\} \\ &\quad + E\{(\mathbf{y}_n^* \otimes \mathbf{1}_\nu)(\mathbf{1}_\nu \otimes \mathbf{y}_n)^H\} \\ &\quad \odot E\{(\mathbf{1}_\nu \otimes \mathbf{y}_n)(\mathbf{y}_n^* \otimes \mathbf{1}_\nu)^H\}. \end{aligned} \quad (64)$$

Next, we will simplify (64) term by term.

According to data model (10), the first term becomes [27]

$$\mathbf{K}_y = (\mathbf{H}^* \otimes \mathbf{H}) \mathbf{K}_w (\mathbf{H}^* \otimes \mathbf{H})^H + \mathbf{K}_v. \quad (65)$$

For Gaussian noise,  $\mathbf{K}_v = \mathbf{0}$ , whereas for  $L$  independent inputs

$$\begin{aligned} \mathbf{K}_w &= \sum_{i=1}^L \kappa_i (\mathbf{e}_{L,i} \otimes \mathbf{e}_{L,i})(\mathbf{e}_{L,i} \otimes \mathbf{e}_{L,i})^T \\ &= (\mathbf{I}_L \square \mathbf{I}_L) \text{diag}\{\kappa_1, \dots, \kappa_L\} (\mathbf{I}_L \square \mathbf{I}_L)^T \end{aligned} \quad (66)$$

where  $\kappa_i$  is the kurtosis (fourth-order auto-cumulant) of the  $i$ th input. If all inputs have the same kurtosis  $\kappa_{4w}$ , after substituting (66) into (65) and applying (4), we obtain

$$\mathbf{K}_y = \kappa_{4w} (\mathbf{H}^* \square \mathbf{H})(\mathbf{H}^* \square \mathbf{H})^H. \quad (67)$$

The second term of (64) can be easily observed to be  $\mathbf{r} \mathbf{r}^H$ . The third term is simplified as  $\mathbf{R}^* \otimes \mathbf{R}$ . The last term vanishes for complex variables [22]. For real variables, its first half becomes

$$\begin{aligned} E\{(\mathbf{y}_n \otimes \mathbf{1}_\nu)(\mathbf{1}_\nu^T \otimes \mathbf{y}_n^T)\} &= E\{(\mathbf{I}_\nu \mathbf{y}_n \otimes \mathbf{1}_\nu)(\mathbf{1}_\nu^T \otimes \mathbf{y}_n^T \mathbf{I}_\nu)\} \\ &= E\{(\mathbf{I}_\nu \otimes \mathbf{1}_\nu)(\mathbf{y}_n \otimes \mathbf{1}) (\mathbf{1} \otimes \mathbf{y}_n^T) (\mathbf{1}_\nu^T \otimes \mathbf{I}_\nu)\} \\ &= (\mathbf{I}_\nu \otimes \mathbf{1}_\nu) E\{\mathbf{y}_n \mathbf{y}_n^T\} (\mathbf{1}_\nu^T \otimes \mathbf{I}_\nu) \\ &= (\mathbf{I}_\nu \otimes \mathbf{1}_\nu) \mathbf{R} (\mathbf{1}_\nu^T \otimes \mathbf{I}_\nu) \end{aligned} \quad (68)$$

where (3) has been applied to obtain the second equality, and both vector  $\mathbf{1}_\nu$  and scalar 1 are involved in the second equality. Similarly, the second half of the last term of (64) can be simplified as

$$E\{(\mathbf{1}_\nu \otimes \mathbf{y}_n)(\mathbf{y}_n^T \otimes \mathbf{1}_\nu^T)\} = (\mathbf{1}_\nu \otimes \mathbf{I}_\nu) \mathbf{R} (\mathbf{I}_\nu \otimes \mathbf{1}_\nu^T). \quad (69)$$

Combining all previously derived results, we have, for real variables

$$\begin{aligned} E\{(\mathbf{y}_n^* \otimes \mathbf{y}_n)(\mathbf{y}_n^T \otimes \mathbf{y}_n^H)\} &= \kappa_{4w} (\mathbf{H} \square \mathbf{H})(\mathbf{H} \square \mathbf{H})^T + \mathbf{r} \mathbf{r}^T + \mathbf{R} \otimes \mathbf{R} \\ &\quad + [(\mathbf{I}_\nu \otimes \mathbf{1}_\nu) \mathbf{R} (\mathbf{1}_\nu^T \otimes \mathbf{I}_\nu)] \odot (\mathbf{1}_\nu \otimes \mathbf{I}_\nu) \mathbf{R} (\mathbf{I}_\nu \otimes \mathbf{1}_\nu^T) \end{aligned} \quad (70)$$

whereas for complex variables

$$E\{(\mathbf{y}_n^* \otimes \mathbf{y}_n)(\mathbf{y}_n^T \otimes \mathbf{y}_n^H)\} = \kappa_w (\mathbf{H}^* \square \mathbf{H})(\mathbf{H}^* \square \mathbf{H})^H + \mathbf{r} \mathbf{r}^H + \mathbf{R}^* \otimes \mathbf{R}. \quad (71)$$

Therefore, (37) and (38) follow immediately after (62), (70), and (71) are considered.  $\square$

APPENDIX B  
DERIVATION OF SOME EXPECTED VALUES  
FOR THE ZF RECEIVER

*Derivation of  $E\{\delta\mathbf{H}\mathbf{Z}\delta\mathbf{H}^H\}$*

Denote the  $(a,b)$ th element of  $\mathbf{Z}$  by  $z_{a,b}$ . According to (41), we can write  $\delta\mathbf{H}\mathbf{Z}\delta\mathbf{H}^H$  as

$$\delta\mathbf{H}\mathbf{Z}\delta\mathbf{H}^H = \sum_{a,b=1}^L z_{a,b} \delta\mathbf{h}_a \delta\mathbf{h}_b^H.$$

Therefore, we have

$$E\{\delta\mathbf{H}\mathbf{Z}\delta\mathbf{H}^H\} = \sum_{a,b=1}^L z_{a,b} E\{\delta\mathbf{h}_a \delta\mathbf{h}_b^H\} \quad (72)$$

where  $E\{\delta\mathbf{h}_a \delta\mathbf{h}_b^H\}$  is given by (45).

*Derivation of  $E\{\delta\mathbf{H}^H \mathbf{Z} \delta\mathbf{H}\}$*

From (41), the  $(a,b)$ th element of  $\delta\mathbf{H}^H \mathbf{Z} \delta\mathbf{H}$  is a scalar  $\delta\mathbf{h}_a^H \mathbf{Z} \delta\mathbf{h}_b$ . It can be written as  $\text{tr}(\delta\mathbf{h}_b \delta\mathbf{h}_a^H \mathbf{Z})$ . Therefore, the  $(a,b)$ th element of  $E\{\delta\mathbf{H}^H \mathbf{Z} \delta\mathbf{H}\}$  is given by

$$\text{tr} \left( E \left\{ \delta\mathbf{h}_b \delta\mathbf{h}_a^H \right\} \mathbf{Z} \right) \quad (73)$$

where  $E\{\delta\mathbf{h}_b \delta\mathbf{h}_a^H\}$  can be obtained according to (45).

*Derivation of  $E\{\delta\mathbf{H}\mathbf{Z}\delta\mathbf{H}\}$*

It is clear that  $E\{\delta\mathbf{H}\mathbf{Z}\delta\mathbf{H}\}$  is zero for a complex system. Therefore, we focus on a real system next.

Denote the  $a$ th row of  $\mathbf{Z}$  as  $z_a^T$ . Then,  $\delta\mathbf{H}\mathbf{Z}$  can be written as  $\sum_{a=1}^L \delta\mathbf{h}_a z_a^T$ . Therefore

$$\delta\mathbf{H}\mathbf{Z}\delta\mathbf{H} = \left[ \sum_{a=1}^L \delta\mathbf{h}_a z_a^T \delta\mathbf{h}_1, \dots, \sum_{a=1}^L \delta\mathbf{h}_a z_a^T \delta\mathbf{h}_L \right].$$

The  $b$ th column of this matrix is  $\sum_{a=1}^L \delta\mathbf{h}_a z_a^T \delta\mathbf{h}_b$  or, equivalently,  $\sum_{a=1}^L \delta\mathbf{h}_a \delta\mathbf{h}_b^T z_a$ . Then, the  $b$ th column of  $E\{\delta\mathbf{H}\mathbf{Z}\delta\mathbf{H}\}$  becomes

$$\sum_{a=1}^L E \left\{ \delta\mathbf{h}_a \delta\mathbf{h}_b^T \right\} z_a$$

where  $E\{\delta\mathbf{h}_a \delta\mathbf{h}_b^T\}$  is obtained from (45) after replacing the Hermitian by transpose.  $\square$

APPENDIX C

SIMPLIFICATION OF  $E\{\delta\mathbf{R}\mathbf{Z}\delta\mathbf{r}\}$  AND  $E\{\delta\mathbf{r}^H \mathbf{Z} \delta\mathbf{R}\}$  FOR THE MMSE RECEIVER

First, it is observed that if we take a Hermitian operation on  $E\{\delta\mathbf{R}\mathbf{Z}\delta\mathbf{r}\}$ , then we obtain a form  $E\{\delta\mathbf{r}^H \mathbf{Z} \delta\mathbf{R}\}$ . Thus, we only focus on simplification of  $E\{\delta\mathbf{R}\mathbf{Z}\delta\mathbf{r}\}$ . Since results

from both Propositions 1 and 2 provide statistics of data covariance estimation, there exist two different approaches to simplify  $E\{\delta\mathbf{R}\mathbf{Z}\delta\mathbf{r}\}$ : 1) Express  $\delta\mathbf{r}$  by  $\delta\mathbf{R}$  and apply Proposition 2; 2) express  $\delta\mathbf{R}$  by  $\delta\mathbf{r}$ , and apply Proposition 1. Here, we simply pick up one of them without a specific reason, e.g., the first one.

In  $E\{\delta\mathbf{R}\mathbf{Z}\delta\mathbf{r}\}$ , matrix  $\mathbf{Z}$  has  $\nu$  rows and  $\nu^2$  columns. Let us partition  $\mathbf{Z}$  into  $\nu$  equal-size block columns

$$\mathbf{Z} = \left[ \mathbf{Z}^{(1)}, \dots, \mathbf{Z}^{(\nu)} \right].$$

Each sub-block has  $\nu$  column vectors. The  $a$ th sub-block is denoted as  $\mathbf{Z}^{(a)}$ . After intentionally introducing two identity matrices and applying (2) to  $\delta\mathbf{r}$  as

$$\delta\mathbf{r} = \text{vec}(\delta\mathbf{R}\mathbf{I}_\nu \mathbf{I}_\nu) = (\mathbf{I}_\nu \otimes \delta\mathbf{R}) \text{vec}(\mathbf{I}_\nu)$$

and expressing the  $a$ th entry of  $\text{vec}(\mathbf{I}_\nu)$  by  $\mathbf{e}_{\nu,a}$ , we obtain

$$\delta\mathbf{R}\mathbf{Z}\delta\mathbf{r} = [\delta\mathbf{R}\mathbf{Z}^{(1)}, \dots, \delta\mathbf{R}\mathbf{Z}^{(\nu)}] \delta\mathbf{r} = \sum_{a=1}^{\nu} \delta\mathbf{R}\mathbf{Z}^{(a)} \delta\mathbf{R}\mathbf{e}_{\nu,a}.$$

Therefore

$$E\{\delta\mathbf{R}\mathbf{Z}\delta\mathbf{r}\} = \sum_{a=1}^{\nu} E\{\delta\mathbf{R}\mathbf{Z}^{(a)} \delta\mathbf{R}\} \mathbf{e}_{\nu,a}$$

where  $E\{\delta\mathbf{R}\mathbf{Z}^{(a)} \delta\mathbf{R}\}$  can be obtained from Proposition 2.  $\square$

REFERENCES

- [1] *Physical Layer Standard for cdma2000 Standards for Spread Spectrum Systems—TIA/EIA/IS-2000.2-A*, Mar. 2000. Telecommun. Industry Association TIA, TIA/EIA Interim Stand..
- [2] 3GPP TS 25.2-Series (Physical Layer) (2001, Mar.). [Online]. Available: <http://www.3gpp.org>; <http://www.3gpp2.org>; <http://www.itu.int/itu-t>
- [3] A. Viterbi, *Principles of Spread Spectrum Communication*. Reading, MA: Addison-Wesley, 1995.
- [4] W. Lu and R. Berezdivin, "Technologies on fourth-generation mobile communications," *IEEE Wireless Commun.*, vol. 40, Apr. 2002.
- [5] S. Verdu, *Multuser Detection*. New York: Cambridge Univ. Press, 1998.
- [6] S. Bensley and B. Aazhang, "Subspace-based channel estimation for code division multiple access communication Systems," *IEEE Trans. Commun.*, vol. 44, pp. 1009–1020, Aug. 1996.
- [7] M. Torlak and G. Xu, "Blind multiuser channel estimation in asynchronous CDMA systems," *IEEE Trans. Signal Processing*, vol. 45, pp. 137–147, Jan. 1997.
- [8] X. Wang and H. Poor, "Blind multiuser detection: A subspace approach," *IEEE Trans. Inform. Theory*, vol. 44, pp. 677–690, Mar. 1998.
- [9] —, "Blind equalization and multiuser detection in dispersive CDMA channels," *IEEE Trans. Commun.*, vol. 46, pp. 91–103, Jan. 1998.
- [10] M. Tsatsanis and Z. Xu, "Performance analysis of minimum variance CDMA receivers," *IEEE Trans. Signal Processing*, vol. 46, pp. 3014–3022, Nov. 1998.
- [11] Z. Xu and M. Tsatsanis, "Blind adaptive algorithms for minimum variance CDMA receivers," *IEEE Trans. Commun.*, vol. 49, pp. 180–194, Jan. 2001.
- [12] Z. Tian, K. Bell, and H. Van Trees, "Robust constrained linear receivers for CDMA wireless systems," *IEEE Trans. Signal Processing*, vol. 49, pp. 1510–1522, July 2001.
- [13] Z. Xu, "Improved constraint for multipath mitigation in constrained MOE multiuser detection," *J. Commun. Networks*, vol. 3, no. 3, pp. 249–256, Sept. 2001.

- [14] —, “Further study on MOE-Based multiuser detection in unknown multipath,” in *EURASIP J. Applied Signal Process.: Multiuser Detection Blind Estimation*, Dec. 2002, pp. 1377–1386.
- [15] Z. Xu, P. Liu, and X. Wang, “Toward closing the gap between MOE and subspace methods,” in *Proc. Asilomar Conf. Signals, Syst., Comput.*, Nov. 2002, pp. 689–693.
- [16] —, “Blind multiuser detection: From MOE to subspace methods,” *IEEE Trans. Signal Processing*, vol. 52, pp. 510–524, Feb. 2004.
- [17] Z. Xu, “Asymptotically near-optimal blind estimation of multipath CDMA channels,” *IEEE Trans. Signal Processing*, vol. 49, pp. 2003–2017, Sept. 2001.
- [18] S. D. Gray, M. Kocic, and D. Brady, “Multiuser detection in mismatched multiple-access channels,” *IEEE Trans. Commun.*, vol. 43, pp. 3080–3089, Dec. 1995.
- [19] Z. Xu, “Asymptotic performance of subspace methods for synchronous multirate CDMA systems,” *IEEE Trans. Signal Processing*, vol. 50, pp. 2015–2026, Aug. 2002.
- [20] —, “Perturbation analysis for subspace decomposition with applications in subspace-based algorithms,” *IEEE Trans. Signal Processing*, vol. 50, pp. 2820–2830, Nov. 2002.
- [21] —, “On the second-order statistics of the weighted sample covariance matrix,” *IEEE Trans. Signal Processing*, vol. 51, pp. 527–534, Feb. 2003.
- [22] A. J. van der Veen, “Statistical performance analysis of the algebraic constant modulus algorithm,” *IEEE Trans. Signal Processing*, vol. 50, pp. 3083–3097, Dec. 2002.
- [23] P. Lancaster and M. Tismenetsky, *The Theory of Matrices*, Second ed. San Diego, CA: Academic, 1985.
- [24] H. L. Van Trees, *Optimum Array Processing. Part IV of Detection, Estimation and Modulation Theory*. New York: Wiley, 2002. App. A.
- [25] T. Krauss, W. Hillery, and M. Zoltowski, “Downlink specific linear equalization for frequency selective CDMA cellular systems,” *J. VLSI Signal Process. Syst. Signal, Image, Video Technol.*, vol. 30, no. 1–3, pp. 143–161, Jan.–Mar. 2002.
- [26] A. H. Madsen and X. Wang, “Performance of blind and group-blind multiuser detectors,” *IEEE Trans. Inform. Theory*, vol. 48, pp. 1849–1872, July 2002.
- [27] G. B. Giannakis, Y. Hua, P. Stoica, and L. Tong, *Signal Processing Advances in Wireless & Mobile Communications: Trends in Single- and Multi-User Systems—Volume 2*. Englewood Cliffs, NJ: Prentice-Hall, 2001, ch. 3.



**Zhengyuan Xu** (S'97–M'99–SM'02) received the B.S. and M.S. degrees in electronic engineering from Tsinghua University, Beijing, China, in 1989 and 1991, respectively, and the Ph.D. degree in electrical engineering from Stevens Institute of Technology, Hoboken, NJ, in 1999.

From 1991 to 1996, he worked as an engineer and department manager at the Tsinghua Unisplendour Group Corp., Tsinghua University. Since 1999, he has been with the Department of Electrical Engineering, University of California, Riverside, as an assistant professor. His current research interests include detection and estimation theory, spread spectrum and ultra-wideband wireless technology, advanced signal processing for multiuser communications, and *ad hoc* and wireless sensor networking.

Dr. Xu received the Outstanding Student Award and the Motorola Scholarship from Tsinghua University and the Peskin Award from Stevens Institute of Technology. He also received the Academic Senate Research Award and the Regents' Faculty Award from University of California, Riverside. He is a Member of the IEEE Signal Processing Society's Technical Committee on Signal Processing for Communications, an Associate Editor for the IEEE TRANSACTIONS ON VEHICULAR TECHNOLOGY and the IEEE COMMUNICATIONS LETTERS.